

Red variables in the OGLE-II database. II. Comparison of the Large and Small Magellanic Clouds

L. L. Kiss^{*†} and T. R. Bedding

School of Physics, University of Sydney 2006, Australia

Accepted ... Received ...; in original form ..

ABSTRACT

We present period-luminosity relations for more than 3,200 red variable stars in the Small Magellanic Cloud observed in the second phase of the Optical Gravitational Lensing Experiment (OGLE-II). Periods of multiply-periodic light curve solutions combined with the single-epoch 2MASS JHK_S magnitudes, reveal very similar distributions to those for the Large Magellanic Cloud in Paper I. The main features include four pulsating Asymptotic Giant Branch (AGB) ridges, three distinct short-period sequences below the tip of the Red Giant Branch and two long-period sequences of ambiguous origin. We derive a relative distance modulus of the Clouds from the period-luminosity distributions for all stars of $\Delta\mu_0 = 0.44$ mag, which is in good agreement with recent independent results. The tip of the Red Giant Branch shows a colour and metallicity dependence that is in excellent agreement with the empirical results for globular clusters. We conclude that most variable stars below the TRGB are indeed RGB stars.

Key words: stars: late-type – stars: variables – stars: oscillations – stars: AGB and post-AGB

1 INTRODUCTION

The period-luminosity (P-L) relations of long period variables on the AGB are well documented for the Large Magellanic Cloud. Observations have revealed not only that Mira variables follow a tight near-infrared P-L relation (Glass & Lloyd Evans 1981, 2003; Feast et al. 1989), but also that semiregular variables pulsating in overtone modes follow distinct and well-defined P-L relations (Wood et al. 1999, Wood 2000). In recent years, there has been strong interest in pulsating red giants, which is reflected in the increasing number of independent analyses of large photometric databases (Cioni et al. 2001, 2003, Noda et al. 2002, Lebzelter et al. 2002, Glass & Schultheis 2003, Kiss & Bedding 2003, Ita et al. 2003, Groenewegen 2004).

An interesting by-product was the recognition of a distinct and very numerous group of red variables below the tip of the Red Giant Branch (TRGB). First, Ita et al. (2002) noted that the luminosity function (LF) of red giant variable stars in the LMC shows a sharp feature at the expected brightness of the TRGB. Earlier, Alves et al. (1998) and Wood (2000) suggested that thermally pulsing AGB stars can mimic a two-peaked luminosity function, and thus the LF shape alone is not sufficient to establish the existence of TRGB variables. However, we have shown in Paper I (Kiss & Bedding 2003) that the LMC period-luminosity relations for stars above and

below the TRGB show a relative period shift that is consistent with evolutionary temperature difference between RGB and AGB stars. This result has since been confirmed by Ita et al. (2003). The possibility of observable pulsations in RGB stars therefore seems to be well established, providing a new area for asteroseismological considerations. In this Letter we provide further evidence for extragalactic RGB variables through a comparative analysis of red variables in the Small Magellanic Cloud (SMC).

Red giant pulsators in the SMC have a far less extensive literature than those of the LMC. The largest pre-microlensing datasets for the SMC were published by Wood et al. (1981), Lloyd Evans et al. (1988) and Sebo & Wood (1994), all consisting of a few dozen variables at most. Microlensing surveys (MACHO, EROS, OGLE) have changed the situation by discovering thousands of red variables. Based on the extensive new datasets, it has become possible to compare the Magellanic Clouds and the Galactic Bulge in search for metallicity effects on red giant pulsations and P-L relations. Cioni et al. (2003) examined MACHO light curves of 458 LPVs in the SMC that were detected by the Infrared Space Observatory. They found very similar P-L sequences to those in the LMC and confirmed the relative overabundance of carbon-rich Mira stars (as recognized first by Lloyd Evans et al. 1988). The most extensive analysis to date is that of Ita et al. (2003), who determined the dominant period for 2,927 variables in the SMC using OGLE-II data and constructed P-L relations using single-epoch SIRIUS JHK survey data. Beside finding the same distributions as those in Paper I, Ita et al. (2003) derived zero-point differences of the P-L relations of

* E-mail: laszlo@physics.usyd.edu.au

† On leave from University of Szeged, Hungary

about 0.1 mag. Some differences were also noted recently by Cioni et al. (2003) for the Magellanic Clouds and by Glass & Schultheis (2003) for the Galactic Bulge and the Magellanic Clouds. The latter investigators found both slightly different slopes and different absolute magnitude ranges for the overtone P-L sequences. These interesting results depend on the assumed distances to each of the different P-L datasets. Here we concentrate on the multi-wavelength luminosity functions to sort out the distance issue, and examine the implications concerning the RGB pulsations.

2 DATA ANALYSIS

The basis of our analysis is the catalogue of OGLE-II (Udalski et al. 1997) data spanning four years from 1997 to 2000 (Zebrun et al. 2001). Of the total 7 square degrees of the OGLE Magellanic Cloud fields, about 2.5 square degrees were observed in the SMC. The observations were analysed by the OGLE team using a modification of the Difference Image Analysis (Alard & Lupton, 1998, Wozniak 2000), which is the most advanced method available for detecting small variations in crowded fields (see, e.g., Bonanos & Stanek 2003).

Typical light curves in the SMC consist of 280 points distributed over $\sim 1,100$ days. Compared to the LMC, where individual datasets covered slightly more than 1,200 days in 400 points, this means a reduced accuracy in period determination. We consider our periods reliable up to about 400–500 days, for which at least two cycles were observed.

The data were analysed in the same manner as in Paper I. To summarise, we performed the following steps:

(i) We cross-correlated the 15,038 OGLE-II variable stars in the SMC with the 2MASS All-Sky Point Source Catalog¹; within a search radius of $1''$ we found 10,361 stars with JHK_S magnitudes. The tight constraint on coordinates ensured that we identified the infrared counterparts unambiguously.

(ii) After excluding duplicates (< 10), we selected red giants according to the $J - K_S$ colour. The applied threshold was $J - K_S > 0.9$ mag. We have also excluded all stars with $K_S > 14$ mag because of the strongly increasing errors of 2MASS magnitudes below that limit. The final sample consisted of 3,898 stars.

(iii) We performed a period search on OGLE-II light curves by an iterative Fourier analysis (see Paper I for details), until a four-component harmonic fit was calculated. We kept only those frequencies larger than $8 \times 10^{-4} \text{ d}^{-1}$ ($\sim 1/T_{\text{obs}}$) and with semi-amplitudes larger than 5 mmag.

(iv) The resulting database contains 3,260 stars with 10,009 periods (and amplitudes and phases), the mean I -band magnitude and 2MASS JHK_S single-epoch magnitudes.

Our sample is slightly larger than that of Ita et al. (2003) because of the different selection criteria. A more relevant difference is that we calculated a set of periods for every star, while Ita et al. (2003) determined only one period per star. We found multiple periodicity for the majority of stars (82% of the full sample), which can, therefore, be identified as common behaviour in red giants. There must be, of course, a fraction of spurious or physically unrelated periods, which need a more sophisticated method for identification and exclusion from future analyses.

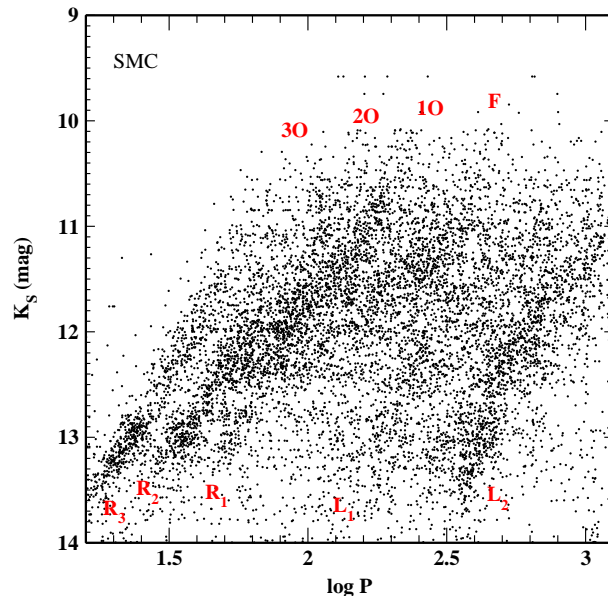


Figure 1. P-L relations for red giants in the SMC (10,009 periods for 3,260 stars).

3 DISCUSSION

We present the resulting P-L diagram in Fig 1. At first glance, the shape and extension of distributions are very similar to those we found for the LMC: (i) there is a noticeable drop of point density at $K_S \approx 12.70$ mag, located close to the tip of the RGB (Cioni et al. 2000); (ii) above the tip, there are four pulsating AGB sequences, which in the LMC were identified by Wood (2000) as stars pulsating in the fundamental (F), first (10), second (20) and third (30) overtone modes (he labelled them as sequences C, B and A which, however, does not account for the fact that there are four ridges clearly distinguishable in the OGLE-II data); (iii) below the tip, there are three distinct sequences in the short-period range ($P < 60$ days), of which R_2 and R_3 are continuations of 20 and 30; there might be a slight horizontal shift, similar to that found in the LMC (Paper I), but the ridges are less well defined, due to the smaller number of stars, so the possible period shift between 30 – R_3 and between 20 – R_2 is hardly measurable. The sequence R_1 , just as for the LMC, lies somewhere between the extrapolated 10 and F ridges; (iv) for longer periods, there are two sequences, L_1 and L_2 , in the same relative position to the other ridges as in the LMC. Their interpretation is ambiguous; Wood (2000) suggested L_1 (=E in his paper) contains eclipsing binary variables, while L_2 (=D) may consist of pulsating stars with unknown excitation mechanism or non-spherical stars with rotationally induced variations (Olivier & Wood 2003, Wood 2004).

Although multiperiodicity is a common feature, there is a remarkable difference above and below the tip of the RGB: for $K_S < 12.7$ mag, 95%, while for $K_S > 12.7$, only 62% of the light curves resulted in multiple periods. This, however, only reflects the fact that amplitudes below the TRGB strongly decreases towards fainter magnitudes (see Sect. 3.3), thus the fixed 5 mmag amplitude threshold may be too high for most of the periods (if they exist). In addition, we stress there is not any noticeable change between the resulting P-L distributions when plotting every star just once using the strongest period or using all periods with amplitudes exceeding a certain threshold (or even plotting every star just once with the second strongest period).

¹ <http://irsa.ipac.caltech.edu>

Table 1. Relative distance moduli and extinctions. $\Delta\mu$ is the mean vertical distance between the P-L images; ΔA_X refers to the differential extinction in the X band, while $\Delta\mu_0$ is the dereddened relative distance modulus. $\Delta E(B - V) = 0.085$ (Westerlund 1997) and $\Delta A_V = 0.26$ mag were assumed. The uncertainty in $\Delta\mu$ is about ± 0.05 mag.

Band	$\Delta\mu$	ΔA_X	$\Delta\mu_0$
I	0.25	0.16	0.41
J	0.35	0.07	0.42
H	0.40	0.05	0.45
K_S	0.43	0.03	0.46
mean:			0.44

3.1 The relative distance modulus of the Clouds

In the case of such complex structures as the P-L distributions of red variables in the Magellanic Clouds, it is difficult to measure the vertical distance between the P-L ridges directly. It has been a more common approach to assume a relative distance modulus and overplot the relations with the purpose of comparison, either in a simplified functional form (see Fig. 11 in Glass & Schultheis 2003) or showing the full observational data (Fig. 10 in Ita et al. 2003). Here we follow a different approach to show that, assuming a negligible mean zero-point difference for the set of relations, one can get consistent relative distance moduli and extinctions of the Clouds in all four photometric bands (IJK_S), which will be used later to characterize the dips of the luminosity functions.

Instead of a visual examination of overplotted data, we calculated the cross-correlation functions of smoothed images of the P-L ridges (being the sharpest in K_S and the least-defined in I). For this, we converted the scatter diagrams (Fig. 1 and Fig. 1 in Paper I) to 500×500 pixel images as follows. The x-axis covered $\log P$ between 1.2 and 3.1 (3.8×10^{-3} dex/pixel), while the y-axis covered 5 magnitudes, where the exact range depended on the studied band (e.g., from 9 mag to 14 mag in K_S). This way one pixel in vertical direction corresponds to 0.01 mag. Every pixel “intensity” value was set to the total number of stars in a 21×21 pixel mask, centered on the actual pixel. This masking worked as a boxcar smoothing procedure, which produced clear images of the P-L ridges. The cross-correlation functions of the IJK_S P-L images were calculated as functions of $\Delta\mu$, and their maxima showed the vertical shifts that give the best overlap of the images. In order to minimize the effects of spurious periods, we kept only stars with $\log P < 2.6$ (i.e. $P < 1$ year); in other words, we used only 360×500 pixel sub-images.

The resulting shifts are presented in the second column of Table 1. There is a strong wavelength dependence, which can be explained by the differential reddening. The average $E(B - V)$ for the LMC and the SMC are 0.15 mag and 0.065 mag, respectively (Westerlund 1997), which can be translated to ΔA_X differential extinction by adopting $R_V = 3.1$ and the relative extinction coefficients (A_X/A_V) in Schlegel et al. (1998).

As can be seen in Table 1, the dereddened relative distance moduli agree well within the error bars ($\sim \pm 0.05$ mag in every band). Similar agreement exists for recently published results; for instance, Cioni et al. (2000) determined $\Delta\mu = 0.44$ mag. On the other hand, Ita et al. (2003) adopted $\Delta\mu = 0.49$ mag, while Glass & Schultheis (2003) used 0.50 mag. In the rest of the paper we adopt 0.44 mag with an estimated ± 0.03 mag random error.

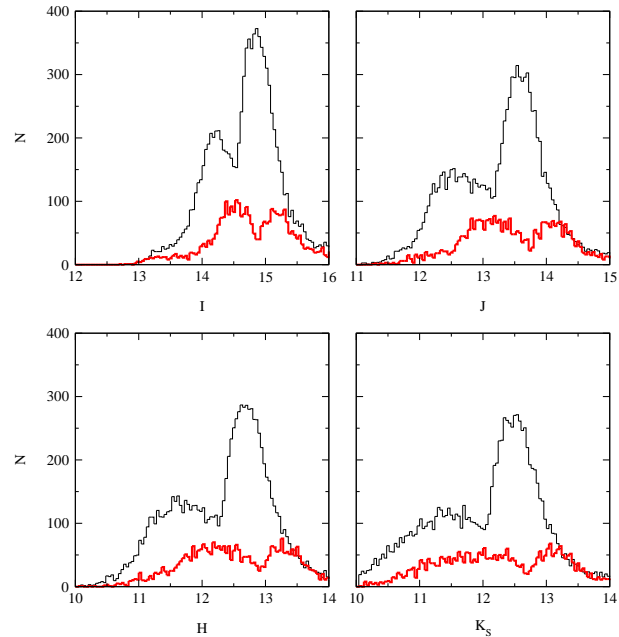


Figure 2. Stellar magnitude distributions for OGLE-II variables in the SMC (thick red line) and in the LMC (thin black line), normalized by the survey area.

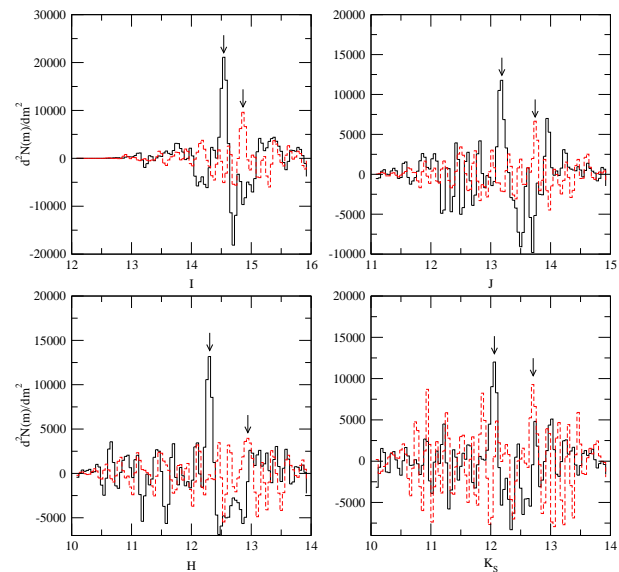


Figure 3. The second derivatives of the smoothed luminosity functions. The arrows point to the maxima for the LMC (solid lines) and the SMC (dashed lines).

3.2 The luminosity functions and the tip of the RGB

In Fig. 2 we plot luminosity functions in all four bands of the OGLE-II+2MASS database: the thin solid line shows the LMC data after correction for the different survey areas (4.5 square degrees for the LMC vs. 2.5 square degrees for the SMC); the thick solid line denotes the SMC LF.

Both Clouds have double-peaked LFs with similar shapes and wavelength dependences. The exact overlap of the faint ends of the SMC and area-normalized LMC distributions in IJK_S shows that there is a severe sensitivity cut-off for $J > 14.2$ mag, $H >$

Table 2. Summary of TRGB magnitude values (the uncertainty is about 0.04 mag). C2000 refers to TRGB values in Cioni et al. (2000).

Band	LMC LF dip	SMC LF dip	LMC f''_{obs}	SMC f''_{obs}	LMC (C2000)	SMC (C2000)
<i>I</i>	14.56	14.92	14.54	14.85	14.54	14.95
<i>J</i>	13.20	13.79	13.18	13.74	13.17	13.73
<i>H</i>	12.27	12.90	12.30	12.94	–	–
K_S	12.03	12.72	12.06	12.70	11.98	12.62

13.5 and $K_S > 13.3$ mag. On the other hand, the difference for *I* suggests the drop of the OGLE-II detection efficiency occurs at fainter magnitudes, so that the faint limit in our sample is set by 2MASS and not by OGLE.

An interesting point is the changing shape of the AGB peak. It is the narrowest in *I* (where the full-width-at-half-maximum is 0.7 mag) and going toward the redder bands, the stars spread over wider and wider luminosity ranges (the FWHM increases to 2 mag). This can be understood qualitatively in terms of the larger bolometric correction for the brightest and reddest stars (Alvarez et al. 2000), which results in the observed narrower distribution in *I*. We point out the overall similarity of the two AGB LFs, with only minor differences.

The fainter peaks, on the other hand, show quite different behaviour. The FWHM stays essentially constant with wavelength, with slightly narrower distributions for the SMC. Since the RGB luminosity function is increasing monotonically toward fainter magnitudes (Nikolaev & Weinberg 2000), the sharp cut-off in our data is a consequence of the falling detection efficiency in the combined OGLE-II+2MASS database. The dip between the brighter and fainter peaks is very close to the TRGB magnitudes determined by Cioni et al. (2000) from an analysis of about 150,000 objects in the DENIS catalog and that close proximity was interpreted both by Ita et al. (2002) and us in Paper I as the evidence for pulsating RGB stars.

Following the referee’s recommendations, we examined this agreement more closely. Due to the nature of the tip of the RGB, it manifests as an edge in the luminosity function (f_{obs}). Cioni et al. (2000) have shown very thoroughly in their Appendix that making an unbiased estimate of the discontinuity can be very difficult. Previous authors generally determined the position of the peak in f'_{obs} , while Cioni et al. (2000) argued for using f''_{obs} . Adopting their considerations, we determined the second derivatives of smoothed luminosity functions in all bands (Fig. 3). The OGLE-II LFs were smoothed with a Gaussian weight-function (FWHM=0.04 mag) and the derivatives were approximated by the difference ratios.

The positions of maxima are listed in Table 2. For comparison, we also show the dips of the LFs and the TRGB values determined by Cioni et al. (2000). The overall agreement is excellent: most of the differences do not exceed the uncertainties. The largest discrepancy was found in K_S , which can, however, be explained by a ~ 0.1 mag systematic shift between 2MASS and DENIS *K*-magnitudes. Therefore, we conclude the luminosity functions of OGLE-II variables show exactly the same behaviour as, for instance, those of the much larger DENIS Catalogue towards the Magellanic Clouds, which included both variable and non-variable stars.

Additionally, we find a significant wavelength dependence of the TRGB values, which follows exactly the changes observed in the tip of the RGB as a function of metallicity in globular clusters by Ferraro et al. (2000) and Ivanov & Borissova (2002). For

instance, Ferraro et al. (2000) derived $M_K^{\text{tip}} \sim -0.6[\text{Fe}/\text{H}]$, which implies $\Delta K \approx 0.18$ mag, assuming the metallicity differs by a factor of 2 between the Clouds. The observed differences from the second derivatives are 0.19 mag, 0.25 mag and 0.23 mag in *J*, *H* and K_S , respectively (adopting $\Delta\mu_0 = 0.44$ mag and correcting for differential extinctions) and they are also in good agreement with the relations in Fig. 4 of Ivanov & Borissova (2002). In *I* band, the difference is only 0.03 mag, which illustrates the insensitivity of $M_{\text{TRGB}}(I)$ to metallicity and age (Lee et al. 1993).

We interpret these agreements as our last piece of evidence that the dip between the AGB and RGB peaks indeed corresponds to the tip of the RGB. In Paper I, we have also considered the arguments of Alves et al. (1998) and Wood (2000) that all variables below the TRGB are thermally pulsing AGB stars and that their brighter cut-off matches the TRGB by coincidence. With the presented behaviour, this explanation seems to be quite unlikely. Even if there are faint TP-AGB stars below the tip, their fraction must be small compared to first ascent red giants.

3.3 Amplitude distributions

We finish the comparative analysis by presenting the same six slices of the (period, amplitude, K_S magnitude) data cube as were shown for the LMC in Fig. 4 of Paper I. Colours refer to three *J* – K_S colour ranges, enabling a rough classification of stars as “hot”, “warm” and “cool” red giants.

The distributions are similar to those of the LMC in that there is a good correlation between the amplitude and mode of pulsation. For amplitudes larger than 0.04 mag, practically all variables below the TRGB disappear. Furthermore, the colour distribution within any particular P-L ridge follows the same pattern as in the LMC. There are, however, some striking differences. Firstly, there is a relative lack of “warm” stars among the low-amplitude variables of the SMC. There is one blue dot for every 30 dots in the upper left panel; in the LMC, the ratio is 1:10. A similar under-abundance is also visible in the lower panels. Secondly, the lower three panels are dominated by the very red stars with $J - K_S > 1.4$ mag, which are probably carbon stars. For the highest amplitude variables (all with regular Mira-like light curves), there is only a handful of “hot” and “warm” giants, many of which fall below the fiducial Mira P-L by as much as 1.5–2 mag. These “faint Miras” be identified with the dust-enshrouded Mira stars (Wood 1998), since their extinctions increase strongly toward shorter wavelengths, reaching up to 4-6 magnitudes in *I*. Our data illustrate nicely that, despite the fact that carbon-rich Mira stars obey the same P-L relation as the oxygen-rich Miras (Feast et al. 1989), the use of the Mira P-L relation in extragalactic distance measurements must be restricted to the bluest possible Mira stars.

4 CONCLUSIONS

In this paper we presented the results of a period analysis of OGLE-II red variable stars in the SMC. Multiple periodicity has been found for the majority of stars, and can now be identified as common behaviour in pulsating red giants, regardless of the metallicity.

We confirm the existence of distinct P-L relations below the tip of the Red Giant Branch, announced in Paper I for the LMC. Utilizing the overall P-L distributions, we determined multi-wavelength relative distance moduli and extinctions, which support a consistent view that the differential distance modulus of the Clouds is

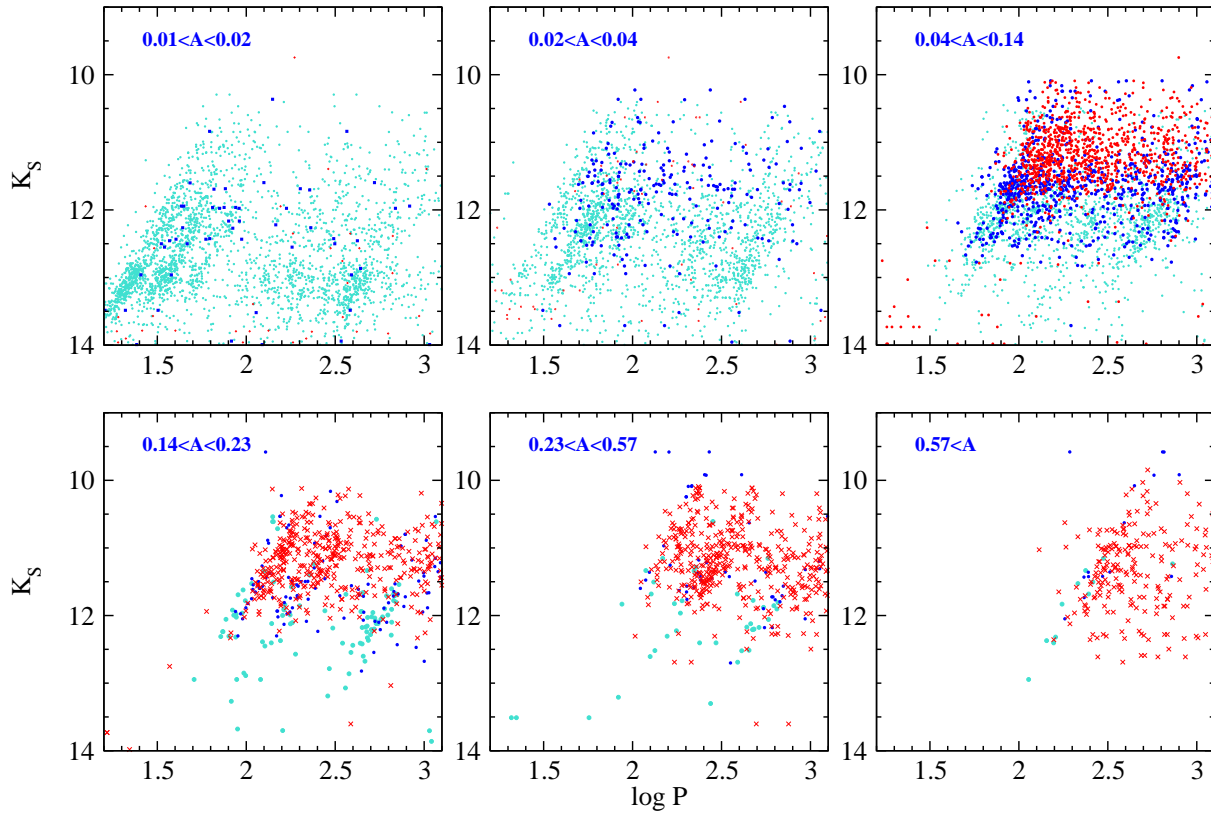


Figure 4. P-L relations in the SMC as function of the full amplitude of modes. Three $J - K_S$ colour ranges were selected to plot in different colours. Turquoise (light gray): $0.9 < J - K_S \leq 1.2$; blue (black): $1.2 < J - K_S \leq 1.4$; red (dark gray): $J - K_S > 1.4$. This figure is available in colour in the on-line version of the journal on *Synergy*. Symbols in the lower panels are drawn larger for improved clarity.

$\Delta\mu_0 \approx 0.44$ mag. The luminosity functions revealed the AGB variables follow very similar distributions in both Clouds. We showed that the dips between the AGB and supposed RGB peaks do indeed correspond to the tip of the RGB (within a few hundredths of a mag). This is also supported by the wavelength-dependent ΔM_{TRGB} (~ 0.20 mag in JHK_S) found as an excess to the relative distance modulus. It is consistent with the metallicity dependence seen among globular clusters and we take this as further evidence that the contamination by thermally pulsing AGB stars is likely to be small.

ACKNOWLEDGMENTS

This work has been supported by the FKFP Grant 0010/2001, OTKA Grant #F043203 and the Australian Research Council. Thanks are due to an anonymous referee, whose suggestions led to significant improvement of the paper. This research has made use of the NASA/IPAC Infrared Science Archive, which is operated by the Jet Propulsion Laboratory, California Institute of Technology, under contract with the National Aeronautics and Space Administration. The NASA ADS Abstract Service was used to access data and references.

REFERENCES

- Alard C., Lupton R.H., 1998, *ApJ*, 503, 325
 Alvarez R., Lançon A., Plez B., Wood P.R., 2000, *A&A*, 353, 322
 Alves D., et al., 1998, In: Proc. of IAU JD24, “Pulsating Stars – Recent Developments in Theory and Observations”, Eds. Takeuti M., Sasselov D.D., Universal Academic Press, Tokyo, 17
 Bonanos A.Z., Stanek K.Z., 2003, *ApJ*, 591, L111
 Cioni M.-R.L., van der Marel R.P., Loup C., Habing H.J., 2000, *A&A*, 359, 601
 Cioni M.-R.L., Marquette J.-B., Loup C. et al., 2001, *A&A*, 377, 945
 Cioni M.-R.L., Blommaert J.A.D.L., Groenewegen M.A.T. et al., 2003, *A&A*, 406, 51
 Feast M.W., Glass I.S., Whitelock P.A., Catchpole R.M., 1989, *MNRAS*, 241, 375
 Ferraro F.R., Montegrifo P., Origlia L., Fusi Pecci F., 2000, *AJ*, 119, 1282
 Glass I.S., Lloyd Evans T., 1981, *Nature*, 291, 303
 Glass I.S., Lloyd Evans T., 2003, *MNRAS*, 343, 67
 Glass I.S., Schultheis M., 2003, *MNRAS*, 345, 39
 Groenewegen M.A.T., 2004, In: Proc. of IAU Coll. 193 “Variable Stars in the Local Group”, ASP Conf. Series, in press
 Ita Y. et al., 2002, *MNRAS*, 337, L31
 Ita Y. et al., 2003, *MNRAS*, in press, (astro-ph/0310083)
 Ivanov V.D., Borissova J., 2002, *A&A*, 390, 937
 Kiss L.L., Bedding T.R., 2003, *MNRAS*, 343, L79 (Paper I)
 Lebzelter T., Schultheis M., Melchior A.L., 2002, *A&A*, 393, 573
 Lee M.G., Freedman W.L., Madore B.F., 1993, *ApJ*, 417, 553
 Lloyd Evans T., Glass I.S., Catchpole R.M., 1988, *MNRAS*, 231, 773
 Nikolaev S., Weinberg M.D., 2000, *ApJ*, 542, 804
 Noda S., Takeuti M., Abe F. et al., 2002, *MNRAS*, 330, 137
 Olivier E.A., Wood P.R., 2003, *ApJ*, 584, 1035
 Schlegel D.J., Finkbeiner D.P., Davis M., 1998, *ApJ*, 500, 525
 Sebo K.M., Wood P.R., 1994, *AJ*, 108, 932
 Udalski A., Kubiak M., Szymanski M., 1997, *Acta Astron.*, 47, 319
 Westerland B.E., 1997, In: *The Magellanic Clouds*, Cambridge Astro-

6 *L. L. Kiss and T. R. Bedding*

- physics Series, 29, 6
- Wood P.R., 1998, *A&A*, 338, 592
- Wood P.R., 2000, *PASA*, 17, 18
- Wood P.R., 2004, In: Proc of IAU Coll. 193 "Variable Stars in the Local Group", ASP Conf. Series, in press
- Wood P.R., Bessell M.S., Fox M.W., 1981, *PASA*, 4, 203
- Wood P.R. et al., 1999, *IAU Symp.* 191, p.151
- Wozniak P.R., 2000, *Acta Astron.*, 50, 421
- Wozniak P.R. et al., 2002, *Acta Astron.*, 52, 129
- Zebrun K. et al., 2001, *Acta Astron.*, 51, 317